Numerical predictions of the anisotropic viscoelastic response of uni-directional fibre composites

M.V. Pathan[a], V.L. Tagarielli[a,*], S.Patsias[b]

[a] *Department of Aeronautics, Imperial College London, South Kensington Campus, SW7 2AZ, UK*

[b] *Rolls-Royce plc, PO Box 31, DE24 8BJ Derby, UK*

Abstract

Finite Element (FE) simulations are conducted to predict the viscoelastic properties of uni-directional (UD) fibre composites. The response of both periodic unit cells and random stochastic volume elements (SVEs) is analysed; the fibres are assumed to behave as linear elastic isotropic solids while the matrix is taken as a linear viscoelastic solid. Monte Carlo analyses are conducted to determine the probability distributions of all viscoelastic properties. Simulations are conducted on SVEs of increasing size in order to determine the size of a representative volume element (RVE); for the fibre volume fractions analysed (0.3 and 0.6), we conclude that elastic properties can be effectively predicted using RVEs of size equal to 24 times the fibre radius, whereas numerical predictions of loss factors require smaller RVEs, of size equal to 12 times the fibre radius. The predictions of the FE simulations are compared to those of existing theories and it is found that the Mori-Tanaka [1] and Lielens [2] models are the most effective in predicting the anisotropic viscoelastic response of the RVE.

Keywords: Composite, Damping, RVE, Finite Element

1. INTRODUCTION

Fibre-reinforced polymers (FRPs) are widely used in industry due to their excellent specific strength and stiffness and also display relatively high material damping compared to metals of similar stiffness. Knowledge of their mechanical properties is essential to achieve optimal

*Corresponding author
Email address: v.tagarielli@imperial.ac.uk (V.L. Tagarielli)

designs with FRPs; while the anisotropic stiffness and strength of FRPs have received great attention from the research community, less studies exist on their damping properties, which are particularly important in aerospace applications. The damping of FRPs is strongly anisotropic and depends on the imposed frequency and temperature; experimental investigations are therefore time-consuming and require specialist equipment. For these reasons, effective numerical and theoretical predictions of the damping properties need to be developed and validated.

Numerous theoretical models exist to predict the elastic response of UD composites; these can be easily extended to the case of viscoelastic materials via the elastic-viscoelastic correspondence principle. In addition to the upper and lower bounds given by the Voigt[3] and Reuss model[4], respectively, Hashin[5] and Hill[6] derived narrower bounds for transversely isotropic composites with isotropic constituents. Hashin and Rosen[7] later derived a predictive model based on a composite cylinder assemblage (CCA). Several predictive models are based on mean-field homogenisation, in which the microfields within each constituent of an inhomogeneous material are approximated by their phase averages by using Eshelby's model[8] . Examples include the Mori-Tanaka [1] model, the Self-Consistent Method (Hill [9]) and Lielens model[2]. Other theoretical models have focused on predictions of viscoelastic properties via extension of previously developed elastic models, the most popular being such as Hashin[10–12], Christensen[13] and Saravanos and Chamis [14].

Several studies attempted validation of the above analytical models via numerical analysis; for example, Chandra et al [15] and Brinson et al [16,17] considered the viscoelastic response of square or hexagonal periodic unit cells; Tsai and Chi [18] pointed out that the damping properties predicted by simulations on unit cell showed are strongly dependent on the choice

of unit cell. Such studies were either limited to a few selected loading cases or they analysed only damping properties but not the elastic response.

Since the spatial distribution of fibres in a UD composite is closer to being random than periodic, it is intuitive to expect that an analysis of a random microstructure should yield more realistic results than the analysis of a periodic unit cell. Several authors have analysed numerically random microstructures; for example Arnold et al. [19] analysed stiffness and strength of UD fibre composites and compared the predictions of periodic unit cells and random microstructures; Gusev et al. [20] analysed random distributions of spherical particles in a continuous matrix to extract its effective elastic properties. Several researchers have focused on the dependence of numerical predictions upon the size of the material volume investigated and gave guidelines for the choice of an effective minimum size. For the case of composites with spherical filler particles, Drugan and Willis [21] found that the elastic properties could be effectively predicted using Representative Volume Elements (RVEs) of size $4R$, where R is the radius of the spherical particle. Trias et al. [22] examined elasticity of UD carbon/epoxy composites and suggested an RVE size greater $50R$.

In the present work, we present a comprehensive numerical analysis of the anisotropic viscoelastic response of a UD fibre composite lamina, simulating both periodic unit cells and random microstructures. For the case of random microstructures we analyse the size-dependence of the FE predictions and their scatter, determining an effective RVE size. Predictions are also compared to existing theoretical approaches with the objective of ranking the effectiveness of different models in predicting the viscoelastic properties.

The outline of the paper is as follows: in Section 2 we review linear viscoelasticity and selected analytical models; the FE simulations are described in detail in Section 3 and the

corresponding numerical results are presented in Section 4. In Section 5 we present and discuss a comparison of numerical and theoretical predictions.

2. REVIEW OF THEORETICAL PREDICTIONS OF THE VISCOELASTIC PROPERTIES

2.1 Response of the constituent materials

Damping in FRPs is primarily due to the viscoelastic nature of the polymeric matrix, since the most commonly used reinforcing fibres are inorganic (e.g. carbon, glass) and their damping properties are negligible. Accordingly, in this work we shall assume a linear elastic response of the fibres.

In normal operating conditions composites experience small deformations; this justifies modelling the polymeric matrix as a linear viscoelastic material. Assuming an isotropic response of the matrix, the constitutive equations of viscoelasticity are given as

$$s_{ij}(t) = \int_{-\infty}^{t} 2G(t-\tau)\frac{de_{ij}}{d\tau}\,d\tau \tag{1}$$

$$p_{ii}(t) = \int_{-\infty}^{t} 3K(t-\tau)\frac{d\phi_{ii}}{d\tau}\,d\tau \tag{2}$$

where s_{ij} and p_{ii} are the components of the deviatoric and hydrostatic stress tensor, respectively, e_{ij} and ϕ_{ij} are the corresponding deviatoric and dilatational strains, $G(t)$ and $K(t)$ are time dependent shear and bulk moduli, respectively [16]. Taking a Fourier Transform of the equations (1) and (2) gives

$$s_{ij}(i\omega t) = 2G^{*}(\omega)e_{ij}(\omega) \tag{3}$$

$$p_{ii}(i\omega t) = 3K^{*}(\omega)\phi_{ii}(\omega). \tag{4}$$

The above equations are analogous to those governing isotropic elasticity but are expressed in the Fourier domain; this correspondence is referred to as the elastic-viscoelastic correspondence principle. $G^*(\omega)$ and $K^*(\omega)$ are Fourier transforms of $G(t)$ and $K(t)$ and can be decomposed in their real and imaginary parts

$$G^*(\omega) = G'(\omega) + iG''(\omega) \tag{5}$$

$$K^*(\omega) = K'(\omega) + iK''(\omega) \tag{6}$$

The real parts $G'(\omega)$ and $K'(\omega)$ are defined as storage moduli, while $G''(\omega)$ and $K''(\omega)$ are the corresponding loss moduli. Loss factors are defined as ratios of the loss modulus to the corresponding storage modulus, i.e.

$$\eta_G = G''/G'; \quad \eta_K = K''/K'. \tag{7}$$

For typical polymers it is typically $\eta_K << \eta_G$, due to the fact that dissipative mechanisms are more pronounced in presence of deviatoric strains. Existing predictive models of the effective elastic properties of fibre composites can be extended to the case of viscoelastic composites by using the elastic-viscoelastic correspondence principle.

The viscoelastic materials can be modelled using normalized Prony series based on the generalized Maxwell model [23] as follows:

$$\frac{G(t)}{G_0} = 1 - \sum_{i=1}^{N} g_i (1 - e^{(-t/\tau_i)}) \tag{8}$$

$$\frac{K(t)}{K_0} = 1 - \sum_{i=1}^{N} k_i (1 - e^{(-t/\tau_i)}) \tag{9}$$

Where G_0 and K_0 are instantaneous shear and bulk moduli, and g_i, k_i and τ_i are the normalized shear and bulk moduli and relaxation time constant of the *i*-th arm of the generalised Maxwell model.

2.2 Response of a transversely isotropic lamina

For a transversely isotropic, uni-directional composite lamina, viscoelasticity can be expressed, in terms of complex engineering constants, as

$$\begin{pmatrix} \varepsilon_{11} \\ \varepsilon_{22} \\ \varepsilon_{33} \\ \gamma_{23} \\ \gamma_{31} \\ \gamma_{12} \end{pmatrix} = \begin{pmatrix} 1/E_{11}^{*} & -\nu_{21}/E_{22}^{*} & -\nu_{21}/E_{22}^{*} & 0 & 0 & 0 \\ -\nu_{12}/E_{11}^{*} & 1/E_{22}^{*} & -\nu_{23}/E_{22}^{*} & 0 & 0 & 0 \\ -\nu_{12}/E_{11}^{*} & -\nu_{23}/E_{22}^{*} & 1/E_{22}^{*} & 0 & 0 & 0 \\ 0 & 0 & 0 & 1/G_{23}^{*} & 0 & 0 \\ 0 & 0 & 0 & 0 & 1/G_{12}^{*} & 0 \\ 0 & 0 & 0 & 0 & 0 & 1/G_{12}^{*} \end{pmatrix} \begin{pmatrix} \sigma_{11} \\ \sigma_{22} \\ \sigma_{33} \\ \tau_{23} \\ \tau_{31} \\ \tau_{12} \end{pmatrix} \tag{10}$$

Five independent loss factors can also be defined for such transversely isotropic material, as

$$\eta_{11} = \frac{E_{11}^{"}}{E_{11}^{'}};\ \ \eta_{22} = \frac{E_{22}^{"}}{E_{22}^{'}};\ \ \eta_{12} = \frac{G_{12}^{"}}{G_{12}^{'}};\ \ \eta_{23} = \frac{G_{23}^{"}}{G_{23}^{'}};\ \ \eta_{\nu_{12}} = \frac{\nu_{12}^{"}}{\nu_{12}^{'}} \tag{11}$$

where, a prime indicates storage properties and a double prime refers to loss properties.

The engineering constants in eqns. (10) and (11) have to be determined experimentally or predicted numerically. Several analytical models exist to predict the values of such engineering constants and loss factors. We shall compare our numerical predictions to those of selected analytical models, namely: direct and inverse rule of mixture [3][4], Hashin's upper and lower bounds [5][6][23][24], Saravanos and Chamis model [14][25], Composite Cylinder Assemblage model [7], Mori-Tanaka model [1] and Lielens interpolative model [2]. The details of these analytical models and the corresponding formulae are provided in Appendix A.

3. NUMERICAL METHODS

We employed the Finite Element (FE) method to simulate the viscoelastic response of a transversely isotropic lamina and to compare the numerical predictions to those of the existing theoretical models described in the previous section. We conducted comprehensive numerical analyses aimed at determining a homogenised viscoelastic tensor for a composite lamina. This was done by analysing the response of three-dimensional random arrays of cylindrical fibres, mimicking the microstructure of a unidirectional fibre composite.

Such microstructure was subjected to four different cyclic loading cases, namely: uniaxial tension-compression in the fibre and transverse directions; transverse and axial shear. A steady state dynamics direct analysis step in the frequency domain was performed in ABAQUS Standard; the macroscopic strains imposed on the RVEs were pure sine waves of amplitude arbitrarily set to 0.01 and varying frequencies; the analysis allowed calculation of the corresponding macroscopic stress histories; such histories were interpreted as phasors and split into two components, in-phase and out-of-phase with respect to the imposed strain. The ratio of the in-phase stress amplitude to the corresponding strain amplitude provided the values of the storage moduli; similarly, the ratio of the out-of-phase stress amplitude to the strain amplitude gave the loss moduli.

The microstructures simulated are random and in general their response is affected by intrinsic scatter; following the definition in [32][a1][a2], the microstructures analysed are statistical Volume Elements (SVEs). Monte Carlo Simulations are performed on each SVE: multiple realisations of the SVEs are simulated, allowing calculation of the cumulative probability distributions of all visco-elastic properties. Monte Carlo analyses are repeated at increasing SVE size in order to determine the size of a Representative Volume Element (RVE).

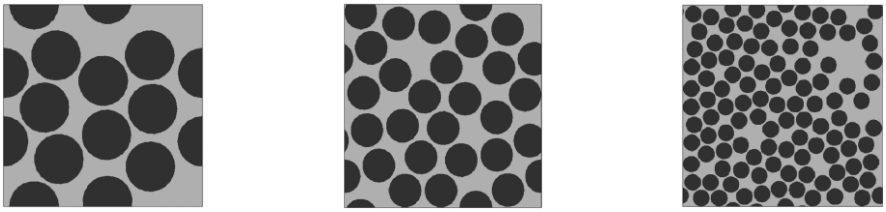

(a) $\delta = 8$ (b) $\delta = 12$ (c) $\delta = 24$

Figure 1: Examples of microstructures at v_f=0.6 for different RVE sizes.

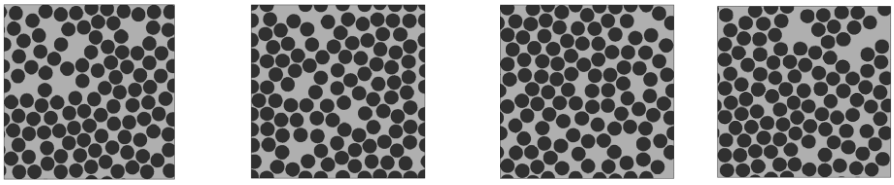

Figure 2: Examples of different realizations of a microstructure with v_f =0.6, δ=24.

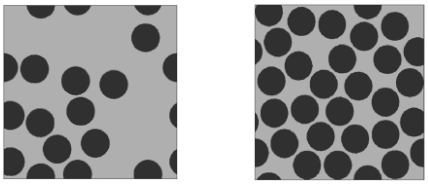

(a) $v_f = 0.3$ (b) $v_f = 0.6$

Figure 3: Examples of microstructures of different volume fractions, for δ=12.

Definitions of an RVE are given, for example, in [33] and [34]. In brief, while SVEs provide only apparent properties of the material, which are in general size-dependent, a RVE is sufficiently large to sample a great number of the microstructural features of a certain material, and this gives a size-independent response, associated to minimal scatter. For the case of a fibre composite, the minimum size of an RVE depends on the volume fraction of fibres as well as on the constitutive response of matrix and fibres. Many authors [22,35] have calculated the minimum RVE size suitable to determine the elastic stiffness constants of unidirectional composites; on the other hand, similar information is lacking for the case of damping properties and our study aims at addressing this. In our study we choose properties of the constituent materials representative of an epoxy resin and glass fibres and we explore

the effect of the fibre volume fraction ($v_f = [0.2 - 0.6]$) on material response and minimum RVE size. For the purpose of comparison, FE analyses are also conducted on square and hexagonal periodic unit cells. The simulations were run using the ABAQUS finite element software.

3.1 Details of the FE models

The microstructures analysed consisted of random arrays of parallel, circular cylindrical fibres of equal diameter. In the plane perpendicular to the fibres the volume elements analysed were squares of side length L, and had thickness *t* in the fibre direction. These were generated via a new algorithm recently proposed by the authors [36], based on optimisation techniques. The microstructures generated were geometrically periodic and they were shown to be effectively random for $\delta = L/R > 7$ (for the case of $v_f = 0.65$; R is the radius of the fibres). Python scripts were used to generate automatically multiple realisations of each SVE, to apply appropriate boundary conditions, to mesh the SVEs and automatically perform the Monte Carlo analyses and extract the relevant outputs.

The microstructures were meshed using a combination of hexahedral and tetrahedral finite elements with linear shape functions (C3D8 and C3D6). A mesh sensitivity study was performed to determine the optimal element size in each loading case and it was found that finite elements of side length less than *R*/4 gave mesh-insensitive predictions for all loading cases.

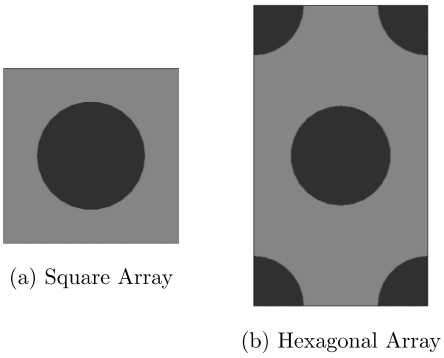

Figure 4: Examples of periodic unit cells with v_f=0.3.

Three selected SVE sizes were analysed, namely δ=8,12 and 24, examples of which are shown in Figs. 2(a)-(c) for the case $v_f = 0.6$; the maximum value of δ was chosen to give *L* comparable to the ply thickness of typical composites. The thickness *t* was shown to have negligible effect on the results, in line with the findings of other authors (e.g. Melro et al. [37]); in our analysis we assumed $t = 4R$. Examples of multiple realisations of the largest SVE ($\delta = 24$, $v_f = 0.6$) are presented in Fig. 3.

Due to the geometric periodicity, the SVEs can only contain an integer number of fibres. The SVE sizes (L) were adjusted in order to achieve the desired volume fractions. The exact SVE sizes (L) are 39.633, 60.54 and 120 μm; in all SVEs it was $R = 5\,\mu\text{m}$.

When conducting Monte Carlo analyses, simulations were repeated *N* times where *N* was 60, 30 and 10 for δ=8,12 and 24, respectively. Examples of SVEs of equal size and different volume fractions are presented in Fig. 4. Figure 5 presents examples of the square and hexagonal unit cells analysed, for the case $v_f = 0.3$.

It is widely accepted that periodic boundary conditions (PBC) are the most appropriate boundary conditions to analyse a geometrically periodic RVE [32,38] and PBCs are imposed on the SVEs analysed here, following, e.g., [39] or [37]. Loading was applied by imposing

nodal displacements on appropriate dummy nodes via the method of macroscopic degrees of freedom, as introduced by Michel et al. [40] and used by Tucker and Liang [30]. Periodic boundary conditions were also imposed for the analysis of periodic unit cells.

The constitutive responses of fibres and matrix were chosen to be representative of a glass/epoxy composite. The fibres were linear elastic isotropic solids while the matrix was modelled as an isotropic, linear viscoelastic solid. For simplicity a one-term Prony series was considered to model the visco-elasticity of the matrix and the same normalised Prony series coefficients and relaxation time constant were used for both deviatoric and volumetric deformation modes. Relevant material constants are provided in Table 1 and 2.

Table 1: Mechanical properties of constituent materials.

	Elastic Modulus GPa	Poisson Ratio
Epoxy	2.76	0.38
Carbon Fibre	50	0.2

Table 2: Prony series coefficients.

	g_i	k_i	τ_i *(sec)*
Epoxy	*0.6*	*0.6*	*20*

4. RESULTS AND DISCUSSION

FE simulations were conducted under steady state harmonic conditions, imposing a macroscopic strain amplitude of 0.01 at frequencies in the range 10^{-8} to10^{2} Hz. The response spectrum for selected viscoelastic constants are given in Fig. 6 for different SVE sizes and for the case $v_f = 0.3$; the results are averages of simulation outputs over the multiple

realizations analysed, and each material property is normalised by the corresponding property of the neat matrix.

As previously reported in literature [32], for all loading cases we detect a size dependence of the elastic constants, however predictions become practically insensitive to size for $\delta \geq 24$. Such size dependence is more pronounced at high loading frequencies; this can be explained as follows: at lower frequencies (and therefore low strain rates) the effective matrix stiffness is very low, corresponding to low strain energy and viscous dissipation in the matrix; predictions become less sensitive to the detail of fibres arrangement, giving a low size-dependence of the predictions. At any frequency, the most substantial size effect is observed for the transverse shear modulus $G_{23}^{'}$. For the case of damping properties (loss moduli), predictions are practically insensitive to size (in the range examined).

We now present the results of the Monte Carlo analyses, examining the probability distributions of the predicted viscoelastic properties, for a selected loading frequency of $\left(2\pi\tau\right)^{-1}$, corresponding to the peak of loss moduli for both the matrix and the composite.

4.1 Results of the Monte Carlo analyses

We begin by presenting the cumulative density functions (CDF) for the predicted axial storage modulus $E_{11}^{'}$. In Fig. 7 we compare the cases of $v_f = 0.3$ and $v_f = 0.6$; for both volume fractions predictions are size independent and associated to minimal scatter, indicating that a small SVE is sufficient to obtain accurate prediction of the axial modulus. Since the fibres are modelled as purely elastic, the corresponding axial loss factors are negligible and are omitted.

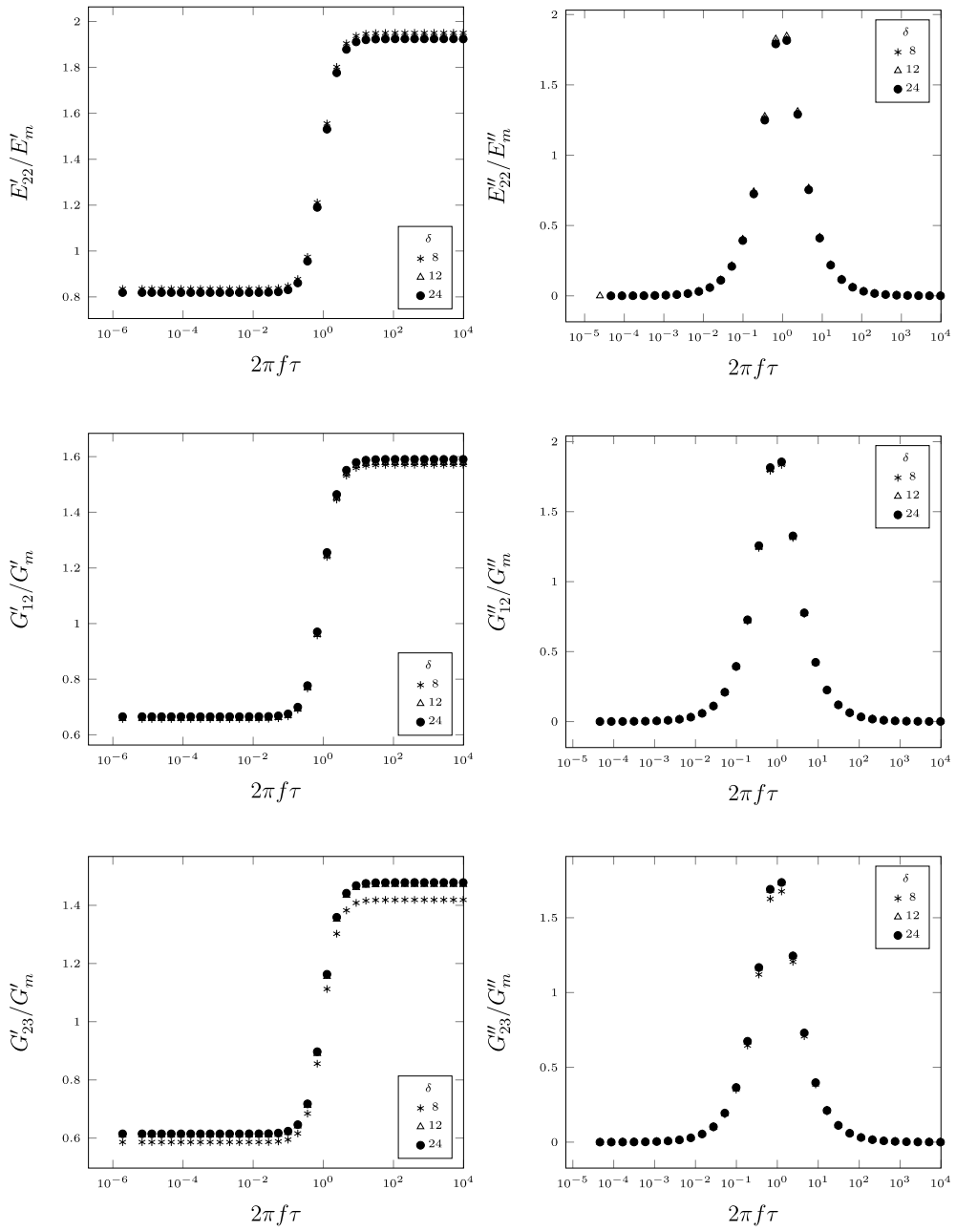

Figure 5: Effect of imposed frequency on the viscoelastic response of SVEs of different size (v_f =0.3).

In Fig. 8 we present a similar comparison for the case of the major Poisson ratio; for this elastic property, we observe that average predictions are size-independent, however they display a substantial scatter, which reduces monotonically with increasing SVE size.

We proceed to analyse the predicted viscoelastic properties of SVEs with $v_f = 0.3$; CDFs of predicted values of the remaining elastic constants ($E_{22}^{'}, G_{12}^{'}, G_{23}^{'}$) and the corresponding loss factors ($\eta_{22}, \eta_{12}, \eta_{23}$) are presented in Fig 9. The scale on the horizontal axis is chosen to

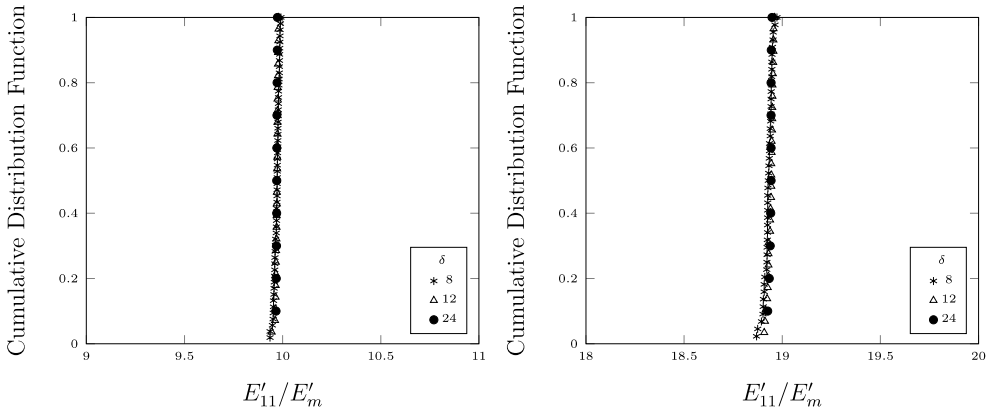

Figure 6: Cumulative distribution functions of E'_{11} for v_f =0.3 (left) and v_f =0.6 (right).

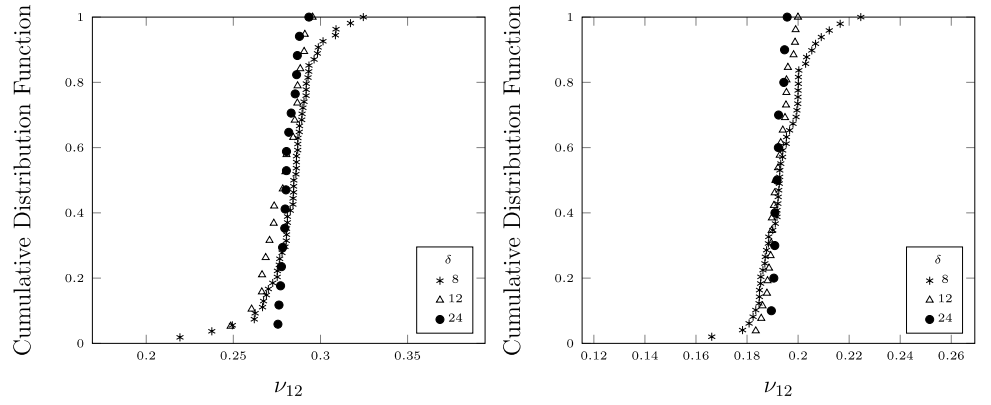

Figure 7: Cumulative distribution functions of ν_{12} for v_f =0.3 (left) and v_f =0.6 (right).

display values from 60% to 140% of the mean, to allow a direct comparison of the predicted scatter for different viscoelastic properties.

For the case of the elastic constants $E_{22}^{'}$ and $G_{12}^{'}$, predicted average values are size-independent, as observed for the case of $E_{11}^{'}$ and ν_{12}; again, as expected, the scatter in the predictions reduces with increasing SVE size. In contrast, predictions for $G_{23}^{'}$ display a

material size effect with the transverse shear modulus increasing with increasing SVE size; the size dependence is however negligible for $\delta \geq 12$. For case of the loss factors, predictions are independent of size and the corresponding scatter is minimal for this volume fraction.

Figure 10 presents identical information as Fig. 9 for the case $v_f = 0.6$. The trends displayed by the predicted material's constant are similar to those observed at the lower volume fraction: all predictions are size-independent with the exception of $G_{23}^{'}$, for which a size effect is detected; the magnitude of such size effect is greater than observed for $v_f = 0.3$. Predictions of the loss factors at this higher volume fraction are associated to a larger scatter than observed at $v_f = 0.3$; however such scatter is substantially less than that determined for the corresponding elastic moduli.

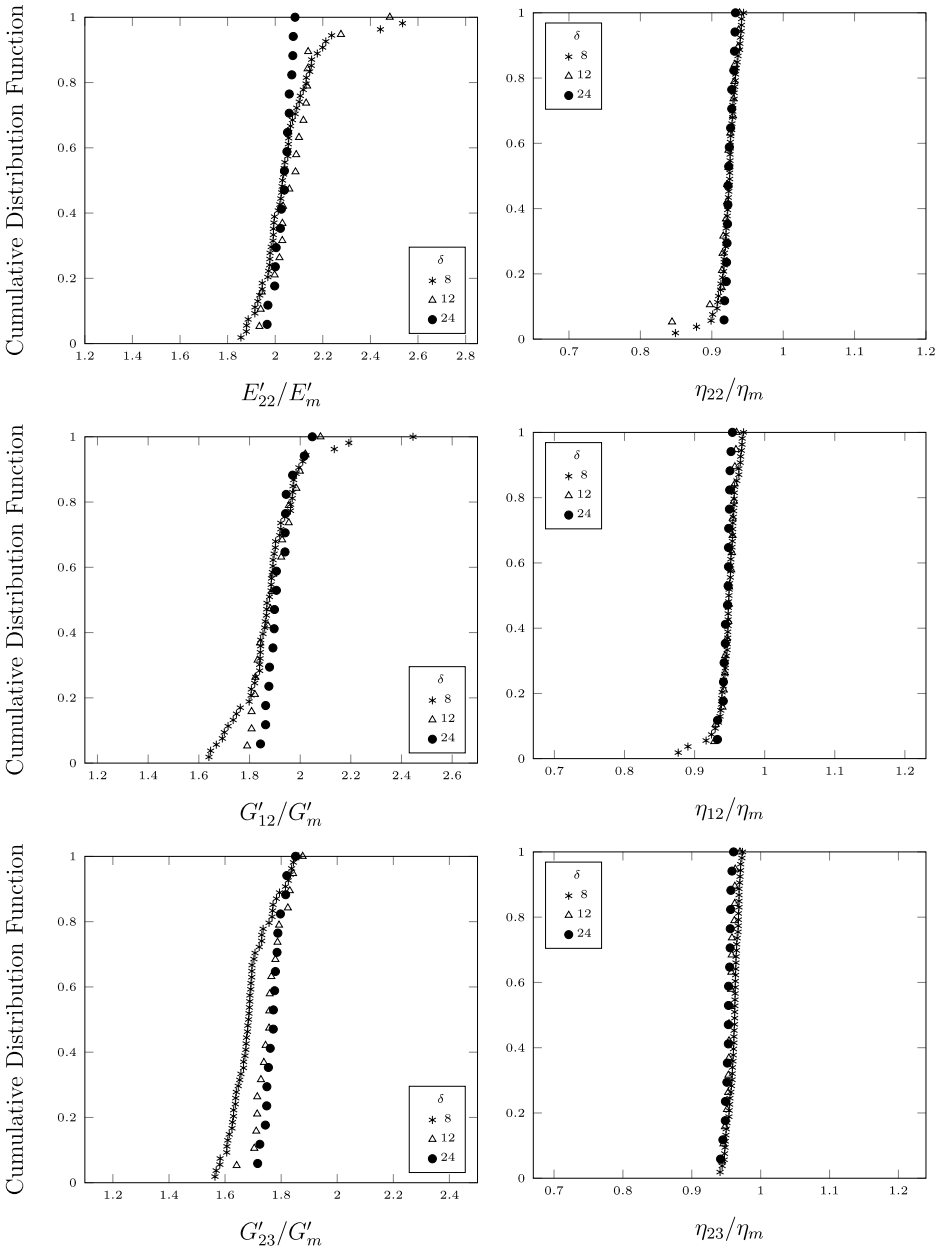

Figure 8: Cumulative distribution functions of viscoelastic properties (v_f =0.3).

For the case $v_f = 0.3$ we performed a best fit of the data to a Gaussian distribution and found, as expected, a very good fit, with Pearson's coefficients higher than 97% for all samples sizes. The parameters of this best fit are as given in Table 3; from this we can deduce that the highest scatter in the predictions is associated with $G_{12}^{'}$, followed by $G_{23}^{'}$, for every SVE size analysed; this indicates that comparatively more number of realisations must be analysed to obtain accurate average predictions of these two shear moduli.

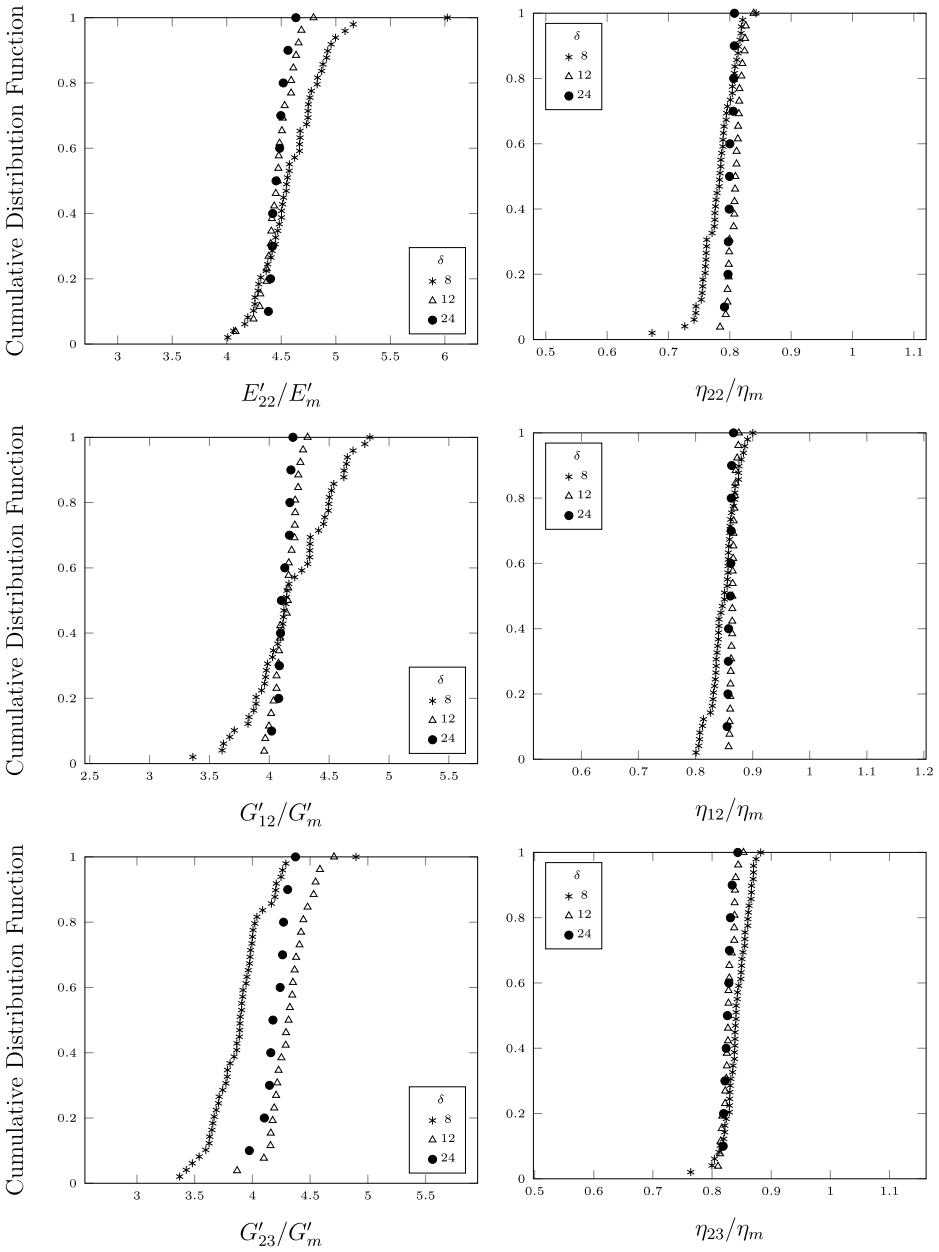

Figure 9: Cumulative distribution functions of viscoelastic properties (v_f =0.6).

4.2 Determination of the minimum RVE size

We now analyse the mean values of the predicted viscoelastic properties and the corresponding 95% confidence interval obtained with SVEs of different size; the objective of this analysis is to determine the minimum SVE size to give size-independent predictions of the mean properties as well as intrinsic scatter below a given tolerance, for a given number of

realisation. In other words, we seek the minimum size of a RVE suitable to determine the viscoelastic properties of a uni-directional fibre composite.

Figure 11 presents numerical predictions for a composite with $v_f = 0.3$; we omit results obtained for the axial modulus $E_{11}^{'}$ and corresponding loss factor η_{11} as predictions for these properties were found to be size independent and associated to minimal scatter in the range of SVE sizes analysed (see Fig. 7). The dashed horizontal lines in each graph represent a range of $\pm 5\%$ around the average predictions of each property, obtained by analysis of the largest microstructure. For all the material properties considered, predicted mean values are practically insensitive to size for $\delta \geq 12$. As expected, the scatter in the predictions reduces monotonically with increasing SVE size. For the case of elastic properties, it is found that for microstructures with $\delta = 24$ the scatter in the predictions is less than $\pm 5\%$; therefore, for the case of 10 repeated simulations on different realisations of the microstructure, $\delta = 24$ represents the minimum RVE size for prediction of the elastic properties. In contrast, the scatter in the predictions of the loss factors is below $\pm 5\%$ for all the SVE sizes analysed; consequently if one is interested in determining only the loss factors, the analysis of a SVE of size $\delta = 8$ will provide sufficiently accurate predictions, for the case of 60 repeated simulations.

Table 3: Curve fit parameters for vf=0.3 (μ Mean, σ Standard Deviation and R Pearson's coefficient).

Property \ L/R	8			12			24		
	μ	σ	R	μ	σ	R	μ	σ	R
E'_{22}/E'_m	2.07	0.183	0.994	2.09	0.127	0.992	2.03	0.036	0.989
G'_{12}/G_m	1.89	0.156	0.993	1.90	0.08	0.991	1.92	0.054	0.987
G'_{23}/G_m	1.69	0.073	0.991	1.76	0.056	0.993	1.77	0.034	0.995
η_{22}/η_m	0.924	0.011	0.996	0.923	0.011	0.989	0.924	0.005	0.989
η_{12}/η_m	0.949	0.010	0.995	0.949	0.009	0.985	0.946	0.006	0.975
η_{23}/η_m	0.962	0.007	0.989	0.956	0.006	0.990	0.953	0.004	0.985

Compare now with the case $v_f = 0.6$, presented in Fig. 12. The trend displayed by the data is similar to that observed for $v_f = 0.3$; again, predicted mean values are scarcely insensitive to size for $\delta \geq 12$, and predictions of elastic properties are associated with scatter of less than $\pm 5\%$ for $\delta = 24$, which therefore represents a suitable RVE size even for this higher volume fraction (for 10 repeated simulations). In contrast, predictions of the loss factors are associated with higher scatter than what observed for $v_f = 0.3$ and therefore the minimum RVE size necessary for accurate predictions of damping properties is $\delta \geq 12$, corresponding to analysis of 30 different realisations. This can be explained observing that for the case $v_f = 0.3$ fibres are more isolated within the polymeric matrix, therefore subject to a strain field scarcely dependent upon fibre position; on the other hand for $v_f = 0.6$ the strain fields around the fibres depend more strongly on the fibre arrangement in each realisation of the SVE, and predictions of the damping properties are expected to be more sensitive to SVE size.

In summary we find that an SVE with $\delta = 24$ is sufficiently large to provide size-independent predictions of the effective elastic properties with an accuracy of $\pm 5\%$ (for the case of 10 repeated simulations). This is in contrast with the value $\delta = 30$ previously reported in the literature by Trias et al. [22] for an accuracy of $\pm 10\%$. These authors analysed a CFRP with $v_f = 0.5$, characterised by a lower stiffness contrast of the constituent materials $\left(E_f / E_m \approx 6\right)$ than that used in the present study $\left(E_f / E_m \approx 30\right)$; it has been shown previously [41,42] that the minimum RVE size (for a given accuracy) increases with increasing stiffness contrast; considering that the volume fractions in the two analyses were

similar, the relatively larger RVE size $\delta = 30$ proposed by [22] must be explained in terms of the different features of the SVEs analysed (these were non-periodic and effectively random only at $\delta \geq 40$) and the type of boundary conditions used.

No data is available, to the best of the authors' knowledge, on the minimum RVE sizes for accurate predictions of loss factors; in our analysis, we find that an SVE of size $\delta \geq 12$ provides size-independent predictions of accuracy $\pm 5\%$, for the case of 30 repeated simulations.

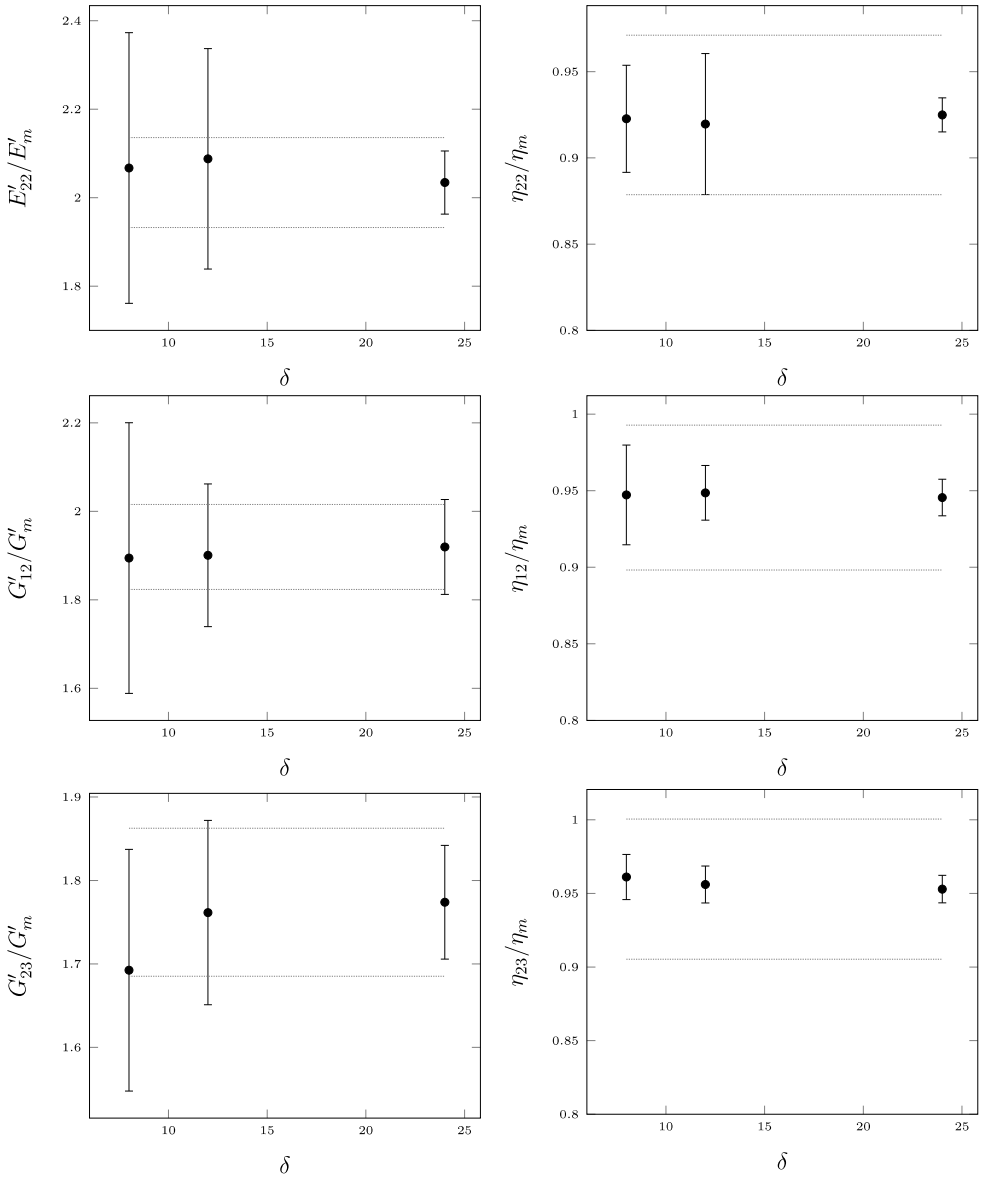

Figure 10: Means and 95% confidence interval of the predictions obtained with different SVE size (vf=0.3).

4.3 Comparison of numerical and theoretical predictions

Finally, we compare theoretical and numerical predictions of the viscoelastic properties. In Fig. 13 we present predictions of all elastic moduli and corresponding loss factors, at increasing fibre volume fractions, for $\delta = 24$ and 10 repeated simulations. The figure includes numerical predictions obtained by FE analysis of square and hexagonal unit cells (Fig. 5), for the purpose of comparison. We observe initially that the theoretical predictions

of Mori-Tanaka, CCA model and Hashin's lower bound are practically coincident for all properties considered.

For case of the longitudinal modulus and corresponding loss factor, all theoretical and numerical predictions coincide; accurate estimates of these properties can be made by any of the numerical or theoretical analyses considered, and these properties are independent of fibre arrangement.

For the transverse Young modulus and loss factor, the predictions obtained by analysis of random RVEs are bounded by those obtained via numerical analysis of periodic unit cells. The theoretical approaches which provide predictions closest to those obtained from the analysis of random RVEs are the models by Lielens and Mori-Tanaka (the latter coincides with Hashin's lower bound and very close to the CCA model). The numerical predictions lie approximately midway between those of Lielens and those of Mori-Tanaka, such that an average of the predictions of these models would give very accurate estimates of both transverse modulus and loss factors.

For the case of axial shear modulus and loss factors, the analysis of RVEs and unit cells provides similar effective properties. Again, numerical predictions obtained via RVE analysis are bounded by the theoretical predictions of Lielens and Mori-Tanaka, with the latter being more effective than the former.

Finally, for the transverse shear modulus and loss factors, the analysis of unit cells gives predictions substantially different from those of random RVEs; in particular, analyses conducted on square unit cells appear to violate Hashin's lower bound, as observed by other authors [37,38,43]. As observed for the transverse Young's modulus and loss factors, predictions from RVE analyses are bounded by the theoretical models of Lielens and Mori-

Tanaka and lie approximately midway between these bounds, such that an average of these theoretical predictions provides accurate estimates of the transverse shear properties.

For all load cases considered, the model by Saravanos and Chamis [14] provides reasonably good estimates of elastic moduli but poor predictions of the loss factors, estimating loss factors which increase with fibre content.

It is expected that the numerical predictions obtained from RVE analyses and presented in this study should be closer to measurements than those obtained from analysing unit cells. Considering that all theoretical approaches presented rely on some approximations, while our RVEs more realistically represent the details of the composite microstructures, we expect the RVE analyses to be more accurate than any of the theoretical models. This should be, however, verified by conducting careful measurements on both composite laminae and their constituent materials (fibres and matrix); this is left as a subject of a future study.

5. CONCLUSIONS

The main conclusions from the numerical studies presented are summarised as follows:

- The predictions of viscoelastic properties obtained from analyses of SVEs display an intrinsic scatter which decrease with increasing fibre volume fraction.
- For an accuracy on the predictions of $\pm 5\%$, it was found that the minimum RVE size for predictions of the elastic properties is $\delta = L / R \geq 24$, for 10 repeated simulations; this value is smaller than previously reported in the literature.
- For predictions of the damping properties with accuracy $\pm 5\%$, the minimum RVE size was found to be $\delta = 12$, for 30 repeated simulations on different realisations of the microstructure; no similar conclusions had been previously reported in the literature.

- The prediction of the transverse shear modulus $G_{23}^{'}$ shows the slowest convergence with increasing SVE size, at any volume fraction; if predictions of $G_{23}^{'}$ are not required, and an accuracy of $\pm 7\%$ is sufficient, an RVE of size $\delta = 12$ (30 repeated simulations) is adequate for volume fraction $v_f = 0.6$.
- A comparison of numerical and theoretical predictions of the viscoelastic properties of UD composites showed that the transverse storage moduli, $E_{22}^{'}$ and $G_{23}^{'}$, and the corresponding loss factors, η_{22} and η_{23}, can be predicted accurately by considering a plain average of the theoretical predictions of Lielens [2] and Mori-Tanaka [1]. For the case of the in-plane shear modulus and corresponding loss factor, $G_{12}^{'}$ and η_{12}, the Mori-Tanaka model provides the most accurate predictions among the theoretical models compared in this study; however this model under-predicts $G_{12}^{'}$ by approximately 15% and over-predicts η_{12} by a similar extent.

6. ACKNOWLEDGEMENTS

This work is part of a collaborative R&T Project "SILOET II Project 10" which is co-funded by Innovate UK and Rolls-Royce plc and carried out by Rolls-Royce plc and Imperial College. The authors are grateful to Rolls-Royce plc for giving permission to publish it.

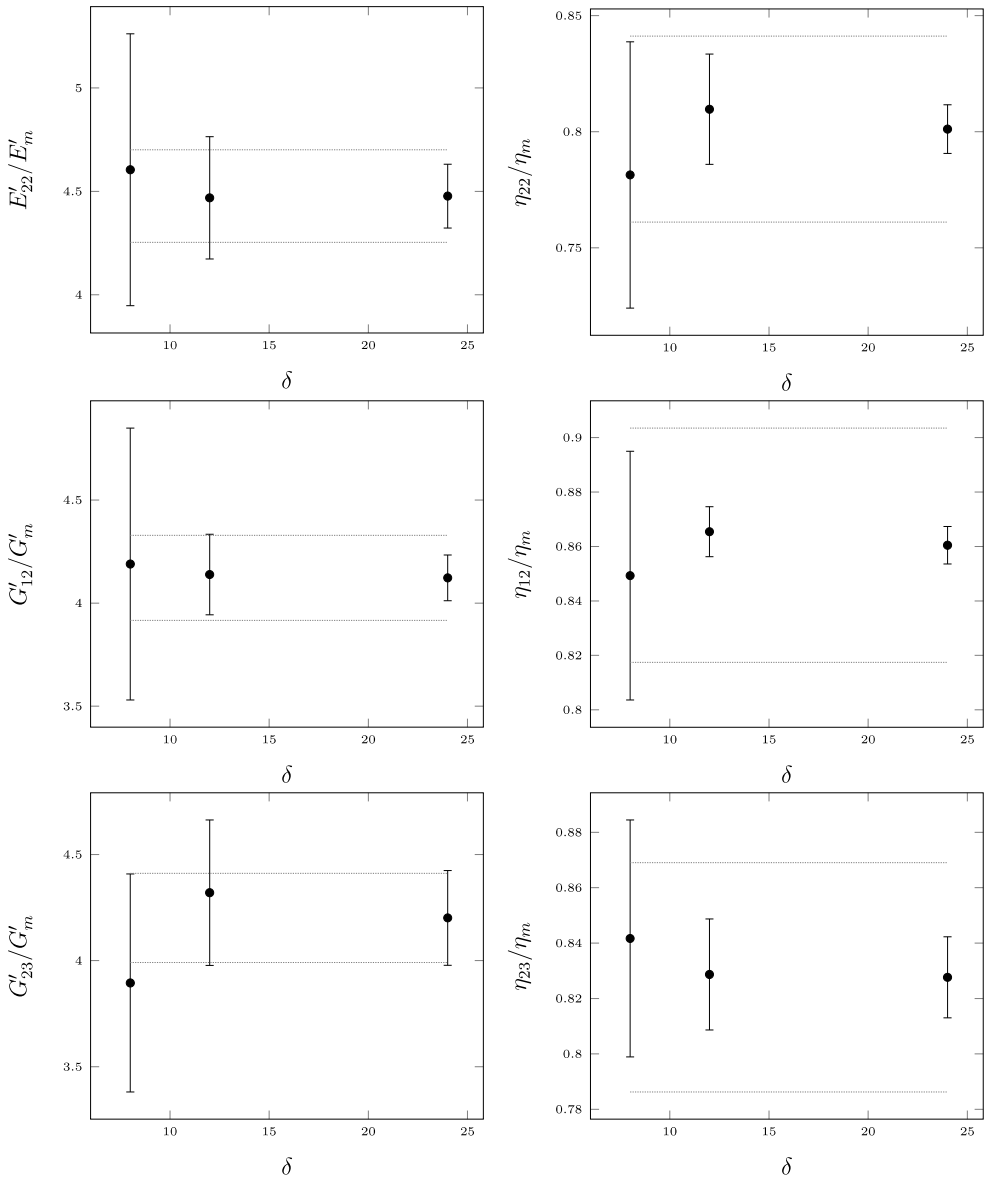

Figure 11: Means and 95% confidence interval of the predictions obtained with different SVE size (vf=0.6).

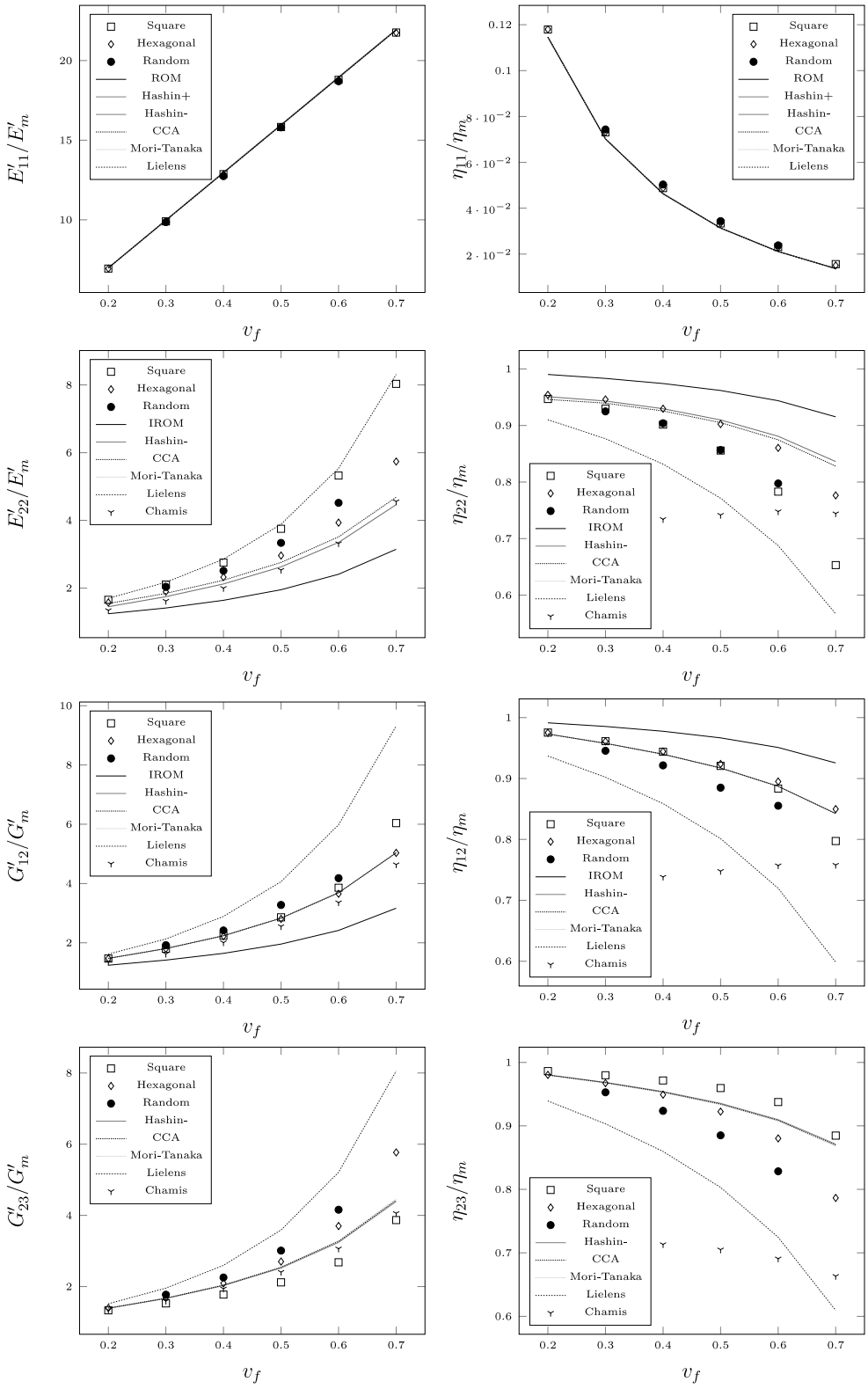

Figure 12: Comparison of theoretical and numerical predictions.

APPENDIX A

In this appendix we review a number of selected analytical models and provide the corresponding predictions for the elastic engineering constants and the corresponding loss factors.

A.1 Voigt and Reuss bounds

Such bounds correspond to assuming either a uniform strain (Voigt [3], providing an upper bound) or a uniform stress (Reuss [4], providing a lower bound) in the different phases of a composite. The effective engineering constants of a two-component composite, must be comprised between the Voigt and Reuss bounds, i.e.

$$\left(\frac{v_f}{P_f^*} + \frac{v_m}{P_m^*} \right)^{-1} \leq P_{ij}^* \leq P_f^* v_f + P_m^* v_m \tag{A1}$$

In the above equation P_{ij}^* denotes a general engineering constant of the composite, P_f^*, P_m^* are the corresponding constant for filler and matrix and v_f, v_m are the associated volume fractions. It is known that the direct rule-of-mixtures (ROM) corresponding to the Voigt bound provides accurate predictions of E_{11}^* and v_{12}^*; on the other hand, the inverse rule-of-mixtures (IROM) given by the Reuss model can effectively predicts E_{22}^* and G_{12}^*.

A.2 Hashin - Hill bounds

Hashin and Shtrikmann [24] developed more accurate bounds for the effective elastic constants of multiphase materials with an arbitrary microstructure. Subsequently Hashin[5] and Hill[6] extended the variational formulation in [23] to the case of transversely isotropic composites. By application of the correspondence principle, the Hashin-Hill bounds for the viscoelastic engineering lamina constants are given as

$$k_m^* + \frac{v_f}{\frac{1}{k_f^* - k_m} + \frac{v_f}{k_f^* + G_m^*}} \le k_{23}^* \le k_f^* + \frac{v_m}{\frac{1}{k_m^* - k_f^*} + \frac{v_f}{k_f^* + G_f^*}} \tag{A2}$$

$$G_m^* + \frac{v_f}{\frac{1}{G_f^* - G_m^*} + \frac{v_m(k_m^* + 2G_m^*)}{2G_m^*(k_m^* + G_m^*)}} \le G_{23}^* \le G_f^* + \frac{v_m}{\frac{1}{G_m^* - G_f^*} + \frac{v_f(k_f^* + 2G_f^*)}{2G_f^*(k_f^* + G_f^*)}} \tag{A3}$$

$$G_m^* + \frac{v_f}{\frac{1}{G_f - G_m^*} + \frac{v_m}{2G_m}} \le G_{12}^* \le G_f^* + \frac{v_m}{\frac{1}{G_m^* - G_f^*} + \frac{v_f}{2G_f^*}} \tag{A4}$$

$$\frac{v_f v_m}{\frac{v_f}{k_m^*} + \frac{v_m}{k_f^*} + \frac{1}{G_m^*}} \le \frac{E_{11}^* - v_f E_f^* - v_m E_m^*}{4(\nu_f - \nu_m)^2} \le \frac{v_f v_m}{\frac{v_f}{k_m^*} + \frac{v_m}{k_f^*} + \frac{1}{G_f^*}} \tag{A5}$$

$$\frac{v_f v_m}{\frac{v_f}{k_m^*} + \frac{v_m}{k_f^*} + \frac{1}{G_m^*}} \le \frac{\nu_{12} - v_f \nu_f - v_m \nu_m}{(\nu_f - \nu_m)(\frac{1}{k_m^*} - \frac{1}{k_f^*})} \le \frac{v_f v_m}{\frac{v_f}{k_m^*} + \frac{v_m}{k_f^*} + \frac{1}{G_f^*}} \tag{A6}$$

Where, k_f^*, k_m^* represent the complex bulk moduli of fibres and matrix and k_{23}^* is the plane strain bulk modulus. Bounds on E_{22}^* can be obtained from manipulation of equations -.

A.3 Saravanos and Chamis model

Saravanos and Chamis [14],[25] constructed micromechanical models to predict stiffness and damping of transversely isotropic lamina. Elastic constants were obtained from analysis of a square unit cell, while loss factors followed from a strain energy method; namely, the authors assumed that loss factors for the composite can be calculated as a weighted average of the loss factors of the constituents, the relative weights being the fractions of strain energy stored

in the two constituents. For the case of isotropic fibres and matrix, Saravanos and Chamis provide

$$E_{11} = v_f E_f + v_m E_m; \quad \eta_{11} = \eta_f v_f \frac{E_f}{E_{11}} + \eta_m v_m \frac{E_m}{E_{11}} \tag{A7}$$

$$E_{22} = (1-\sqrt{v_f})E_m + \frac{\sqrt{v_f}E_m}{1-\sqrt{v_f}(1-\frac{E_m}{E_f})}; \quad \eta_{22} = \eta_f \sqrt{v_f}\frac{E_{22}}{E_f} + \eta_m(1-\sqrt{v_f})\frac{E_{22}}{E_m} \tag{A8}$$

$$G_{12} = (1-\sqrt{v_f})G_m + \frac{\sqrt{v_f}G_m}{1-\sqrt{v_f}(1-\frac{G_m}{E_f})}; \quad \eta_{12} = \eta_{fs} \sqrt{v_f}\frac{G_{12}}{G_f} + \eta_{ms}(1-\sqrt{v_f})\frac{G_{12}}{G_m} \tag{A9}$$

$$G_{23} = \frac{E_{22}}{2(1+v_{23})}; \quad \eta_{23} = \eta_{fs} \sqrt{v_f}\frac{G_{23}}{G_f} + \eta_{ms}(1-\sqrt{v_f})\frac{G_{23}}{G_m} \tag{A10}$$

$$\nu_{23} = \frac{\nu_m}{1-v_f\nu_m} + v_f(\nu_f - \frac{(1-v_f)\nu_m}{1-v_f\nu_m}) \tag{A11}$$

where, η_{fs} and η_{ms} are the shear loss factors of fibres and matrix, respectively.

A.4 Composite Cylinder Assemblage (CCA) model

Hashin and Rosen [7] derived predictions of four engineering constants of a composite lamina, namely longitudinal modulus, longitudinal Poisson's ratio, longitudinal shear modulus and plane strain bulk modulus. The composite is modelled as an assemblage of solid circular cylinders (representing the fibres) surrounded by annular cylindrical regions, representing the matrix. The ratio of fibre diameter and thickness of the annular matrix region is dictated by the volume fraction of the composite. Hashin [11] also developed a similar model based on an assemblage of composite spheres, to predict the properties of composites

with spherical inclusions. The predictions were found to be in good agreement with measurements [10,11]. The effective properties predicted by the CCA model are given below.

$$E_{11}^{*} = v_f E_f^{*} + v_m E_m^{*} + \frac{4 v_f v_m (\nu_f - \nu_m)^2 G_m^{*}}{\frac{v_m G_m^{*}}{K_f^{*} + \frac{G_m^{*}}{3}} + \frac{v_f G_m^{*}}{K_m^{*} + \frac{G_m^{*}}{3}} + 1} \tag{A12}$$

$$\nu_{12}^{*} = v_f \nu_f^{*} + v_m \nu_m^{*} + \frac{v_f v_m (\nu_f - \nu_m)\left(\frac{G_m^{*}}{K_m^{*} + \frac{G_m^{*}}{3}} - \frac{G_m^{*}}{K_f^{*} + \frac{G_f^{*}}{3}}\right)}{\frac{v_m G_m^{*}}{K_f^{*} + \frac{G_f^{*}}{3}} + \frac{v_f G_m^{*}}{K_m^{*} + \frac{G_m^{*}}{3}} + 1} \tag{A13}$$

$$k_{23}^{*} = K_m^{*} + \frac{G_m^{*}}{3} + \frac{v_f}{\frac{1}{\left(K_f^{*} - K_m^{*} + \frac{G_f^{*} - G_m^{*}}{3}\right)} + \frac{v_m}{K_m^{*} + \frac{4 G_m^{*}}{3}}} \tag{A14}$$

$$G_{12}^{*} = G_m^{*} \frac{G_f^{*}(1 + v_f) + G_m^{*} v_m}{G_f^{*} v_m + G_m^{*}(1 + v_f)} \tag{A15}$$

$$G_{23}^{*} = G_m^{*} \frac{\sqrt{B^2 - A C} - B}{A} \tag{A16}$$

where A, B, C are functions of the engineering constants of the constituent materials [11].

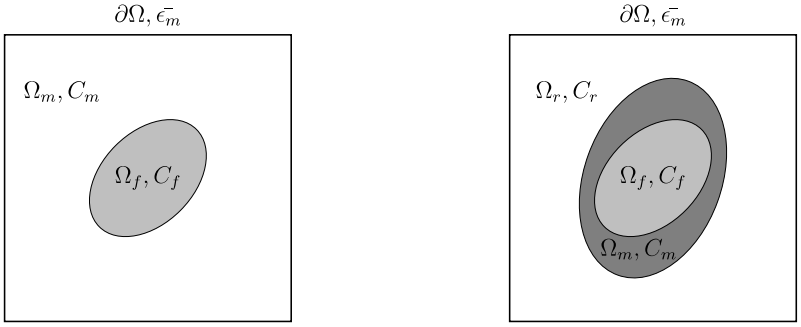

(a) Mori-Tanaka (b) Double inclusion model

Figure A1: Schematic description of different homogenization schemes.

A.5 Mori-Tanaka model

Mori and Tanaka [1] constructed a predictive micromechanical model for the elastic properties of two-phase composites, which was later simplified by Bensvite [26] as it is presented here. Mori and Tanaka introduced inter-particle interaction by adopting an average strain in the matrix phase given by the means of superposition of the far field applied strain ε^0 to a strain perturbation caused by the inhomogeneous microstructure; such average strain in the matrix phase is related to the far-field applied strain by $\bar{\varepsilon}_m = A_{MT}^m \varepsilon^0$ and similarly the average strain in the inclusions is related to the far-field strain by $\bar{\varepsilon}_f = A_{MT}^f \varepsilon^0$.

The modelling approach is sketched in Fig. 1(a); the composite is considered as the assembly of an elliptical inclusion, of stiffness C_f and volume Ω_f, embedded in a large matrix domain of volume Ω_m and stiffness C_m. The relationship between the average strain in the inclusion and in the matrix is given via Eshleby's result [8] for embedded inhomogeneity in an infinite matrix at dilute concentrations, as $\bar{\varepsilon}_f = A_{dil}^f \bar{\varepsilon}_m$, where A_{dil}^f is the strain concentration tensor for dilute concentrations and is given as

$$A_{dil}^f = [I + J_{Eshelby} S_m (C_f - C_m)]^{-1} \tag{A17}$$

Where, I is the identity matrix, $J_{Eshelby}$ is the Eshelby tensor, S_m is the compliance tensor of the matrix material and C_m, C_f are the stiffness tensors for matrix and inclusion materials, respectively. The Eshelby tensor solely depends on the Poisson's ratio and geometry of the inclusion; explicit expressions for this tensor can be found in text by Mura et al. [27]. The Mori-Tanaka strain concentration tensors, A^m_{MT}, A^f_{MT} are given by

$$A^m_{MT} = [(1-v_f)I + v_f A^i_{dil}]^{-1} \tag{A18}$$

$$A^i_{MT} = A_{dil}[(1-v_f)I + v_f A^i_{dil}]^{-1}. \tag{A19}$$

The effective stiffness tensor for the composite is then calculated as

$$C^*_{MT} = \sum v_i C_i A^i_{MT} \tag{A20}$$

Where, the index *i* refers to the various phases of the composite. For two-phase fibre composites, explicit Mori-Tanaka expressions for the effective material constants can be found in Dvorak[28]. The Mori-Tanaka model gives predictions close to those of the Hashin-Hill lower bound in the case of fibres stiffer than the matrix, while it approaches the Hashin-Hill upper bound in the case of compliant fibres in a relatively stiffer matrix; in this case the model is often referred to as the inverse Mori-Tanaka model C^*_{IMT} .

A.7 Double Inclusion Model

A schematic description of this model, suggested by Nemat-Nasser and Hori [29], is given in Fig. 1b. An inclusion of stiffness C_f is surrounded by a shell of matrix material (of stiffness C_m) which in turn is embedded in a reference material of stiffness C_r. The model reduces to the M-T method for the choice of $C_r = C_m$, while it recovers the inverse M-T method for

$C_r = C_f$. Lielens [2] proposed an interpolation between these two limiting cases in terms of a rule-of-mixtures based on the volume fraction of inclusions, as

$$C^*_{Lielens} = [(1 - \frac{v_f + v_f^{\,2}}{2})C^{*-1}_{(MT)} + (\frac{v_f + v_f^{\,2}}{2})C^{*-1}_{(IMT)}]^{-1} \quad \text{(A21)}$$

It was found that the above expression gives accurate predictions of the materials properties over a wide range of volume fractions [30,31].

REFERENCES

[1] T. Mori, H. Tanaka, Average stress in matrix and average elastic energy of materials with misfitting inclusions, Acta Metall. 21 (1973) 571–574.

[2] G. Lielens, Micro-Macro Modeling of Structures Materials, Universite Catholique de Louvain, 1999.

[3] W. Voigt, Ueber die Beziehung zwischen den beiden Elasticitätsconstanten isotroper Körper, Ann. Phys. 274 (1889) 573–587.

[4] A. Reuss, Berechnung der Fließgrenze von Mischkristallen auf Grund der Plastizitätsbedingung für Einkristalle, Z. Für Angew. Math. Mech. 9 (n.d.) 49–58.

[5] Z. Hashin, On elastic behaviour of fibre reinforced materials of arbitrary transverse phase geometry, J. Mech. Phys. Solids. 13 (1965) 119–134.

[6] R. Hill, Theory of mechanical properties of fibre-strengthened materials: I. Elastic behaviour, J. Mech. Phys. Solids. 12 (1964) 199–212.

[7] Z. Hashin, B.W. Rosen, The Elastic Moduli of Fiber-Reinforced Materials, J. Appl. Mech. 31 (1964) 223–232. doi:10.1115/1.3629590.

[8] J.D. Eshelby, The determination of the elastic field of an ellipsoidal inclusion, and related problems, Proc. R. Soc. Lond. Ser. Math. Phys. Eng. Sci. 241 (1957).

[9] R. Hill, A self-consistent mechanics of composite materials, J. Mech. Phys. Solids. 13 (1965) 213–222.

[10] Z.V.I. Hashin, Complex moduli of viscoelastic composites—I. General theory and application to particulate composites, Int. J. Solids Struct. 6 (1970) 539–552.

[11] Z.V.I. Hashin, Complex moduli of viscoelastic composites—II Fibre Reinforced Materials, (n.d.).

[12] Z. Hashin, Damping Characteristics of Fibre Composites, (1972).

[13] R.M. Christensen, Viscoelastic Properties of Heterogeneous Media, J. Mech. Phys. Solids. 17 (1969) 23–41.

[14] D.A. Saravanos, C.C. Chamis, Unified micromechanics of damping for unidirectional fiber reinforced composites, (1989). http://ntrs.nasa.gov/search.jsp?R=19890017548 (accessed July 29, 2014).

[15] R. Chandra, S.P. Singh, K. Gupta, Micromechanical damping models for fiber-reinforced composites: a comparative study, Compos. Part Appl. Sci. Manuf. 33 (2002) 787–796.

[16] L.C. Brinson, W.G. Knauss, Finite element analysis of multiphase viscoelastic solids, J. Appl. Mech. 59 (1992) 730–737.

[17] L.C. Brinson, W.S. Lin, Comparison of micromechanics methods for effective properties of multiphase viscoelastic composites, Compos. Struct. 41 (1998) 353–367.

[18] J.-L. Tsai, Y.-K. Chi, Effect of fiber array on damping behaviors of fiber composites, Compos. Part B Eng. 39 (2008) 1196–1204. doi:10.1016/j.compositesb.2008.03.003.

[19] S.M. Arnold, P. Marek-Jerzy, T.E. Wilt, Influence of fibre architecture on the inelastic response of metal matrix composites, Int. J. Plast. 12 (1996) 507–545.

[20] A.A. Gusev, P.J. Hine, I.M. Ward, Fiber packing and elastic properties of a transversely random unidirectional glass/epoxy composite, Compos. Sci. Technol. 60 (2000) 535–541.
[21] W.J. Drugan, J.R. Willis, A Micromechanical Based Nonlocal Constitutive Equation and Estimates of Representative Volume Element Size for Elastic Composites, J. Mech. Phys. Solids. 44 (1996) 497–524.
[22] D. Trias, J. Costa, A. Turon, J. Hurtado, Determination of the critical size of a statistical representative volume element (SRVE) for carbon reinforced polymers, Acta Mater. 54 (2006) 3471–3484. doi:10.1016/j.actamat.2006.03.042.
[23] M. Kaliske, H. Rothert, Formulation and implementation of three-dimensional viscoelasticity at small and finite strains, Comput. Mech. 19 (1997) 228–239.
[24] Z. Hashin, S. Shtrikman, A Variational Approach to the Theory of the Elastic Behaviour of Multiphase Materials, J.Mech.Phys.Solids. 11 (1963) 127–140.
[25] C. Chamis, Simplified Composite Micromechanics Equations for Hygral, Thermal and Mechanical Properties, NASA Tech. Memo. 83320 (n.d.). http://www.ntrs.nasa.gov/archive/nasa/casi.ntrs.nasa.gov/19830011546_1983011546.pdf (accessed November 5, 2015).
[26] Y. Benveniste, A new approach to the application of Mori-Tanaka theory in composite materials, Mech. Mater. 6 (1987) 147–157.
[27] T. Mura, Micromechanics of Defects in Solids, Springer, 1987.
[28] G. Dvorak, Micromechanics of Composite Materials, Springer Netherlands, 2013.
[29] M. Hori, S. Nemat-Nasser, Double-Inclusion model and overall moduli of multi-phase composites, Mech. Mater. 14 (1993) 189–206.
[30] C.L. Tucker III, E. Liang, Stiffness predictions for unidirectional short-fiber composites: review and evaluation, Compos. Sci. Technol. 59 (1999) 655–671.
[31] E. Ghossein, M. Lévesque, A fully automated numerical tool for a comprehensive validation of homogenization models and its application to spherical particles reinforced composites, Int. J. Solids Struct. 49 (2012) 1387–1398. doi:10.1016/j.ijsolstr.2012.02.021.
[32] T. Kanit, S. Forest, I. Galliet, V. Mounoury, D. Jeulin, Determination of the size of the representative volume element for random composites: statistical and numerical approach, Int. J. Solids Struct. 40 (2003) 3647–3679. doi:10.1016/S0020-7683(03)00143-4.
[33] R. Hill, Elastic properties of reinforced solids: some theoretical principles, J. Mech. Phys. Solids. 11 (1963) 357–372.
[34] I.M. Gitman, H. Askes, L.J. Sluys, Representative volume: Existence and size determination, Eng. Fract. Mech. 74 (2007) 2518–2534. doi:10.1016/j.engfracmech.2006.12.021.
[35] Z.F. Khisaeva, M. Ostoja-Starzewski, On the Size of RVE in Finite Elasticity of Random Composites, J. Elast. 85 (2006) 153–173. doi:10.1007/s10659-006-9076-y.
[36] M.V. Pathan, V. Tagarielli, S. Patsias, Numerical predictions of the anisotropic viscoelastic response of UD fibre composites, (n.d.).

[37] A.R. Melro, P.P. Camanho, S.T. Pinho, Influence of geometrical parameters on the elastic response of unidirectional composite materials, Compos. Struct. 94 (2012) 3223–3231. doi:10.1016/j.compstruct.2012.05.004.
[38] M. Ostoja-Starzewski, Material spatial randomness: From statistical to representative volume element, Probabilistic Eng. Mech. 21 (2006) 112–132. doi:10.1016/j.probengmech.2005.07.007.
[39] E.J. Barbero, Finite element analysis of composite materials, CRC Press, Boca Raton, 2008.
[40] J.C. Michel, H. Moulinec, P. Suquet, Effective properties of composite materials with periodic microstructure: a computational approach, Comput. Methods Appl. Mech. Eng. 172 (1999) 109–143.
[41] M. Ostoja-Starzewski, Random field models of heterogeneous materials, Int. J. Solids Struct. 35 (1998) 2429–2455.
[42] S. Pecullan, L.V. Gibiansky, S. Torquato, Scale effects on the elastic behavior of periodic andhierarchical two-dimensional composites, J. Mech. Phys. Solids. 47 (1999) 1509–1542.
[43] K. Terada, M. Hori, T. Kyoya, N. Kikuchi, Simulation of the multi-scale convergence in computational homogenization approaches, Int. J. Solids Struct. 37 (2000) 2285–2311.